Lateral Fano resonances and Kondo effect in the strong coupling regime of a *T*-coupled quantum dot

R. Franco
Departamento de Física, Universidad Nacional de Colombia, Ciudadela Universidad Nacional, Bogotá, Colombia

M. S. Figueira*
Instituto de Física, Universidade Federal Fluminense (UFF), Avenida Litorânea s/n, 24210-340 Niterói, Rio de Janeiro, Brazil, Caixa Postal 100.093

E. V. Anda
Departamento de Física, Pontificia Universidade Católica do Rio de Janeiro, 22452-970 Rio de Janeiro, Brazil, Caixa Postal 38071
(Received 24 June 2005; revised manuscript received 23 February 2006; published 5 May 2006)

We study the electronic transport through a quantum wire (QW), modeled by a tight-binding linear chain, with a side-coupled quantum dot (QD). We obtain the conductance with a strong Fano antiresonance. The calculated density of states shows that this behavior is associated to a many-body renormalized QD resonant level $\tilde{E}_f$ at the edge of the conduction band (CB) strongly hybridized with the Van Hove singularity of the one-dimensional density of states of the lead. Different from the Fano antiresonances experimentally found when this system is at the Kondo regime, this phenomenon appears above the Kondo temperature. It is due to the quantum interference between the ballistic channel and a thermal activated channel created by the QD resonance at the vicinity of the bottom of the CB.

DOI: 10.1103/PhysRevB.73.195305 PACS number(s): 73.63.Kv, 73.21.La, 71.27.+a, 71.10.Ay

I. INTRODUCTION

The electronic transport through a quantum wire (QW) with a side-coupled quantum dot (QD) has been studied, from the theoretical point of view, by several authors[1–5] and was recently observed experimentally in a quantum wire with a side-coupled dot (*T*-coupled QD).[6] Experiments performed in a single-electron transistor,[7] and by scanning tunneling microscopy on a single magnetic impurity on a metallic surface,[8] showed that the Kondo resonance, predicted theoretically in these systems[9] and experimentally measured,[10] is present simultaneously with a Fano resonance.[11] This resonance appears when there is a quantum interference process in a system consisting of a continuous degenerated spectrum with a discrete level. The interference is produced among the electrons that circulate along the two channels of the system constituted by the discrete level and the continuous band, and gives rise to asymmetric line shapes in the linear conductance as a function of gate voltage. The Fano resonance has been observed in several different geometries of nanoscopic devices when the conditions for the resonance are fulfilled. Examples of such devices are Aharonov-Bohm interferometers,[12] single-electron transistor in a strong[7] or weak coupled regime,[13] and recently the *T*-coupled quantum dot in the presence of magnetic field was proposed as an effective spin filter.[14,15]

In a previous work we studied the Fano resonance in a *T*-coupled quantum dot, for a weak coupling between the quantum dot and the ballistic channel.[5] Now we discuss a kind of Fano resonance that appears in a *T*-coupled QD when the energy level of the QD is located very near the edge of the CB. In this case the Fano resonance is generated by the quantum interference between the ballistic channel and a thermal activated channel created by the QD resonance at one of the edges of the CB.

In Fig. 1 we present a pictorial representation of the quantum wire side-coupled to a quantum dot (*T*-coupled).

We applied the X-boson method,[16,17] for the single impurity case, to describe the transport properties of this system. This is an approximation that is within the spirit of the slave boson formalism. For the sake of simplicity, we take the limit when the Coulomb interaction at the QD is $U \to \infty$. As we analyzed in our previous work,[5] the X-boson approach is not completely reliable at low temperatures in the extreme Kondo regime, because the Friedel sum rule is not completely satisfied. However, the rule is very well fulfilled in the intermediate valence and in the moderate Kondo regime. On the other hand, for temperatures T greater than the Kondo temperature (T_K), while the slave boson approach breaks down at T_K, the X-boson solution evolves to the correct limit at high temperatures.[5] We can say that the X-boson impurity is a reliable approximation to study the intermediate valence regime for all parameters of the model and it is particularly useful to study temperature-dependent properties of the Anderson impurity for $T > T_K$. This is the case of the present

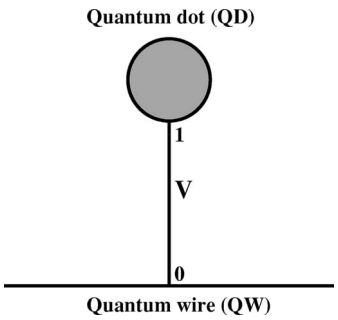

FIG. 1. Pictorial representation of the quantum wire (QW) coupled via hybridization (V) with a side quantum dot (QD).

paper. We are interested to study another kind of Fano resonance, which occurs when $T > T_K$ and the f level is located at the vicinity of the bottom of the conduction band (CB). In this context the X-boson approach is a reliable approximation.

II. MODEL AND GREEN'S FUNCTIONS

A. Model and conductance

We are interested in describing the quantum dot side-coupled to a ballistic channel. The Hamiltonian of the system can be described as an Anderson Hamiltonian and we take the $U=\infty$ limit. It can be written

$$H = H_o + H_{\text{con}}, \tag{1}$$

where H_o describes a tight-binding infinite chain corresponding to the lead, an isolated dot sited at 0 and H_{con} represents the hybridization that connects the quantum dot to the lead:

$$H_o = t \sum_{\sigma, i\neq 0,1} (c^\dagger_{i,\sigma} c_{i-1,\sigma} + \text{H.c.}) + \sum_\sigma E_{f,\sigma} X_{f,\sigma\sigma}, \tag{2}$$

and for the side-coupled dot,

$$H_{\text{con}} = \sum_\sigma [c^\dagger_{0\sigma}(t_{-1} c_{-1,\sigma} + t_{+1} c_{+1,\sigma} + V X_{f,0\sigma} + \text{H.c.})]. \tag{3}$$

We employ the Hubbard operators[18] to project out the double occupation state $|f,2\rangle$, from the local states on the QD (we employ "f" to indicate localized electrons at the QD site). As the X Hubbard operators do not satisfy the usual commutation relations, the diagrammatic methods based on Wick's theorem are not applicable. One has to use product rules instead:[19–21]

$$X_{f,ab} \,.\, X_{f,cd} = \delta_{b,c} X_{f,ad}. \tag{4}$$

The identity decomposition in the reduced space of local states at the QD is given by

$$X_{f,00} + X_{f,\sigma\sigma} + X_{f,\bar{\sigma}\bar{\sigma}} = I, \tag{5}$$

where $\bar{\sigma} = -\sigma$, and the three $X_{f,aa}$ are the projectors into the states $|f,a\rangle$. The occupation numbers on the QD $n_{f,a} = \langle X_{f,aa}\rangle$ satisfy the "completeness" relation

$$n_{f,0} + n_{f,\sigma} + n_{f,\bar{\sigma}} = 1\,. \tag{6}$$

At low temperature and small bias voltage, the electronic transport is coherent and a linear conductance is obtained. Considering the coupling between the chain and the dot $V \ll t$, we can write the conductance as[2]

$$G = \frac{2e^2}{h\rho_c^\sigma(\mu)} \int \left(-\frac{\partial n_F}{\partial \omega}\right) \rho_{00,\sigma}(\omega) d\omega, \tag{7}$$

where n_F is the Fermi distribution and $\rho_{c,\sigma}(\omega) = \frac{-1}{\pi} \text{Im}\, g_c^\sigma(\omega)$ with $g_c^\sigma(\omega)$, being the Green function (GF) of a linear chain that represents the lead. The density of states (DOS) at the dot $\rho_{f\sigma}(\omega)$ is calculated within the X-boson approach through the Green function $G^\sigma_{\text{QD}}(\omega)$. The DOS $\rho_{00,\sigma}(\omega)$ is calculated from the dressed Green function $G^\sigma_{00}(\omega)$ at the wire site 0, and we can write this function in terms of the GF at the QD, $G^\sigma_{\text{QD}}(\omega)$ and the GF of the linear chain $g_c^\sigma(\omega)$ as

$$G^\sigma_{00}(\omega) = [g_c^\sigma(\omega) V]^2 G^\sigma_{\text{QD}}(\omega) + g_c^\sigma(\omega). \tag{8}$$

Considering the lead as a linear tight-binding chain represented by the DOS $\rho_\sigma(\omega) = \frac{1}{\pi\sqrt{4t^2-\omega^2}}$, the X-boson Green's functions are given by[5,16]

$$g_c^\sigma(z) = \langle\langle c_{0,\sigma}; c^\dagger_{0,\sigma}\rangle\rangle_0 = -\frac{1}{\sqrt{z^2-4t^2}}, \tag{9}$$

$$G^\sigma_{\text{QD}}(z) = \langle\langle X_{f,0\sigma}; X^\dagger_{f,0\sigma'}\rangle\rangle_z = \frac{-D_\sigma}{z - \tilde{E}_f - \dfrac{V^2 D_\sigma}{\sqrt{z^2-4t^2}}}, \tag{10}$$

where $z = w + i\eta$, the quantity $D_\sigma = \langle X_{0,0}\rangle + n_f$ is responsible for the correlation in the cumulant X-boson approach[5,16] and $\tilde{E}_f = E_f + \Lambda$, where Λ renormalizes the localized level and is a parameter of the X-boson method given by

$$\Lambda = \frac{-2V}{D_\sigma} \langle c_{i\sigma} X^\dagger_{i,0\sigma}\rangle, \tag{11}$$

where the average in Eq. (11) is calculated through the non-diagonal GF

$$G^\sigma_{00,\text{QD}}(z) = \langle\langle c_{0,\sigma}; X^\dagger_{f,0\sigma}\rangle\rangle_z = G^\sigma_{00}(z) V G^\sigma_{qd}(z). \tag{12}$$

Replacing Eq. (8) in Eq. (7) and neglecting the dependence of $\rho_\sigma(\omega)$ on ω near the chemical potential μ, the Landauer conductance can be written as

$$G = \frac{2e^2}{h}\left[1 - \frac{\pi V^2}{W} I\right]. \tag{13}$$

where

$$I = \int \left(-\frac{\partial n_F}{\partial \omega}\right) \rho_{f\sigma}(\omega) d\omega, \tag{14}$$

and $2t = W$ is the half-width of the tight-binding conduction band.

III. RESULTS

In a previous work,[5] we were interested in studying the interplay between Kondo and Fano effects, where the extra channel at the disposal of the electron to produce the Fano interference phenomenon implied in the Fano antiresonance was provided by the Kondo effect. In our present case the extra channel is provided by the localized electron of the QD that becomes conducting due to thermal promotion. This is the situation where, even in the strong coupling regime, there is a very sharp resonance at the dot, which gives rise to an almost discrete level used by the electrons to go through, creating the possibility of a Fano interference pattern. We will see that the CB amplifies the Fano effect because there is a strong hybridization between the renormalized f level $\tilde{E}_f$ and the one-dimensional Van Hove singularity. The parameter that controls this phenomenon is D_f, the difference in

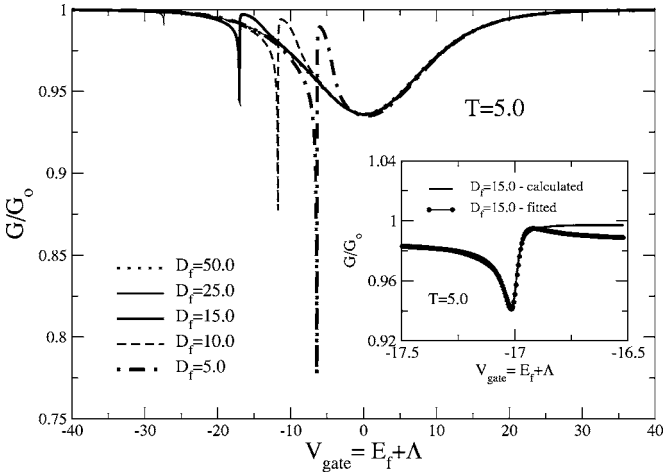

FIG. 2. Conductance G vs $\tilde{E}_f$ for temperature $T=5.0$ and different values of D_f. In the inset we present the adjustment to the Fano formula given by Eqs. (15) and (16).

energy between the chemical potential μ and the edge of the conduction band where the renormalized energy $\tilde{E}_f$ of the QD state is approximately located. All the energy scales are given in units of $\Delta=\frac{\pi V^2}{2W}=1$. We assume the chemical potential to be $\mu=0$.

In Fig. 2 we present the linear conductance G versus $\tilde{E}_f$ for several values of D_f where the temperature is taken to be $T=5.0$. The curve corresponding to $D_f=50.0$ does not present the Fano effect, but as we approximate the Fermi level to the vicinity of the band edge, the Fano resonance appears as it is the case of $D_f=25.0$, and increases more as D_f reduces as we can see in the figure for $D_f=10.0$ and $D_f=5.0$. It is clear that in this last case, as D_f coincides with the temperature of the system, the localized electrons have enough thermal energy to participate in the conduction to give a huge Fano antiresonance.

In Fig. 3 we present, at the same temperature as in Fig. 4, the DOS at the QD $\rho_{\mathrm{QD},\sigma}(\omega)$ at the wire site 0 $\rho_{oo,\sigma}(\omega)$ and with the purpose of comparison, a free chain $\rho_{c,\sigma}(\omega)$ taking

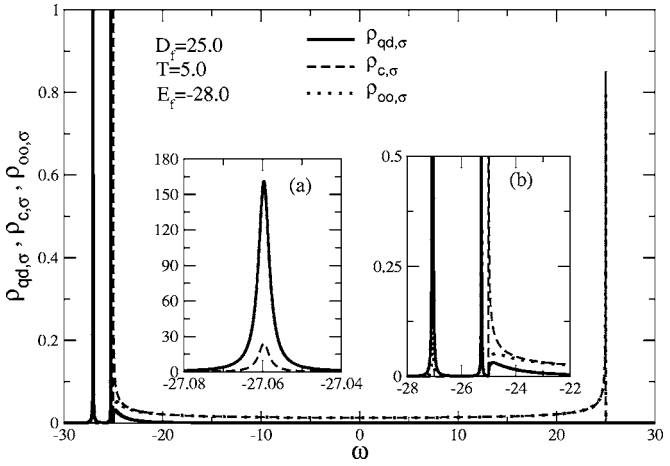

FIG. 3. Density of states associated with the Green's functions of the system. In this case $E_f=-28.0$ and appears a strong f peak at the edge of the conduction band.

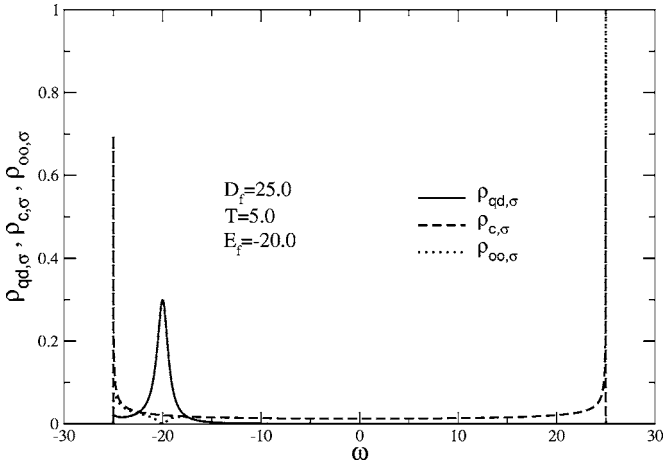

FIG. 4. Density of states associated with the Green's functions of the system. In this case $E_f=-20.0$ and the f peak appears inside the conduction band.

$D_f=25.0$ and $E_f=-28.0$. For these parameters the f level suffers a strong renormalization due to its hybridization with the Van Hove singularity. This produces a strong enhancement of the renormalized peak as indicated by the insets of the figure. The existence of the resonance within the support of the CB creates an alternative interfering channel for the electrons to go along, producing a Fano resonance. However, for this to be operative there should be enough thermal activation so as to permit the electrons populating the edge of the CB to contribute to conduction.

In Fig. 4 we present the DOS associated with the QD $\rho_{\mathrm{QD},\sigma}(\omega)$, the free DOS $\rho_{c,\sigma}(\omega)$ and the DOS at the wire site 0, $\rho_{oo,\sigma}(\omega)$ for the same set of parameters of Fig. 3, but for the case where the Fermi energy ($E_f=-20.0$) is located inside the CB. In this case we can see that $\rho_{QD,\sigma}(\omega)$ loses completely its strong peaked character and there is no Fano resonance. This means that in order to see the resonance Fano effect we are studying it is crucial to have the renormalized f level at the very edge of the CB. In the inset of Fig. 2 we show the Fano character of the lateral resonances by adjusting them to the Fano formula[7,11]

$$G = G_o + G_1 \frac{(E+q)^2}{E^2+1}, \tag{15}$$

$$E = \frac{(E_o - E_r)}{\Gamma/2}; \quad E_o = V_{\mathrm{gate}} = E_f, \tag{16}$$

where G_o in the experimental device corresponds to the noninterfering contribution of the lead and is a smooth function of E_f that can be considered as a constant for the Fano peak, G_1 is the amplitude, E_r is the center of the resonance, and $\Gamma/2$ is their width.[6] As shown in the figure, the results can be almost perfectly adjusted to a Fano shape by adopting the values: $G_o=0.941$, $G_1=0.045$, $\Gamma=0.072$, $q=0.44$, and $E_r=-17.0$.

In Fig. 5 we show the conductance of the system as a function of $\tilde{E}_f$ for different values of the temperature. We expect the lateral Fano structures to disappear as the tem-

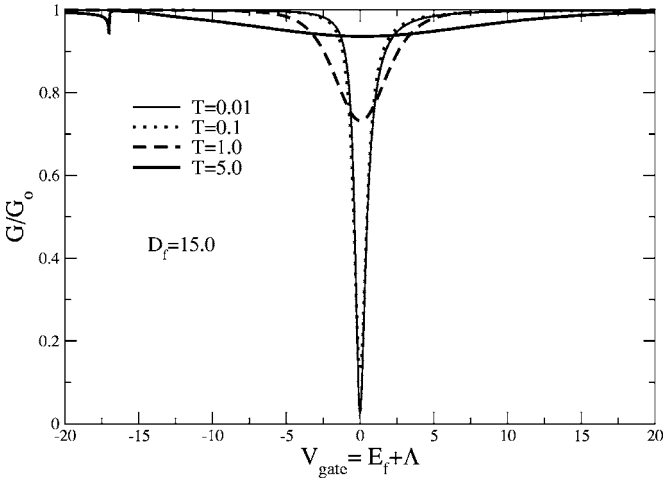

FIG. 5. Conductance G vs $\tilde{E_f}$ for several temperatures (low temperature behavior).

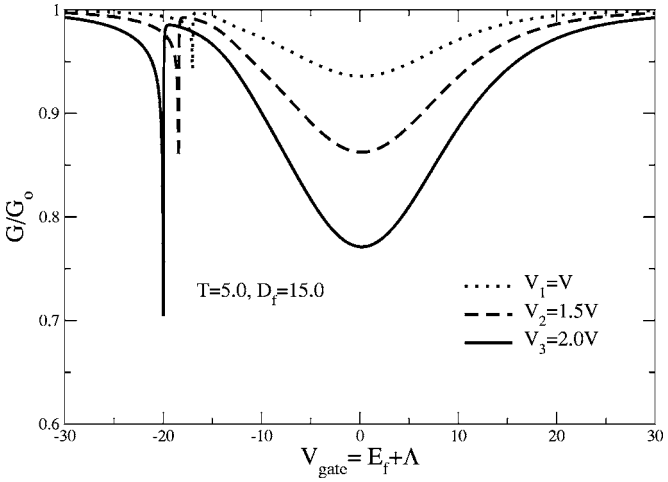

FIG. 7. Conductance G vs $\tilde{E_f}$ for different hybridizations, temperature $T=5.0$ and $D_f=15.0$.

perature is reduced because, in this case, the thermal activated channel is frozen. In fact, as we can see from Fig. 5, as the temperature is reduced from $T=5.0$ to $T=0.01$, the lateral Fano resonances disappear. This behavior is controlled by D_f, the difference in energy between the chemical potential μ and the edge of the CB. As this is a one-level phenomenon, D_f should be less than the interlevel energy of the QD. As discussed below, for low doped semiconductors, this imposes restrictions on the size of the QD that fortunately are experimentally obtainable. Figure 5 depicts as well the emergence of the dip antiresonance, below $T=1.0$, associated with the Kondo resonance at the chemical potential when the temperature is reduced below the Kondo temperature.[1–5]

In Fig. 6 we present the behavior of the lateral resonances in the high temperature limit. When the temperature increases above D_f, the interference between the two channels reduces together with the Fano lateral antiresonance, and simultaneously the background conductance suffers a decrease. A similar result appears in the weak interaction limit when the temperature is increased above the Kondo temperature as it has been experimentally measured.[6] In the inset of the figure we present a detail of the lateral Fano resonance.

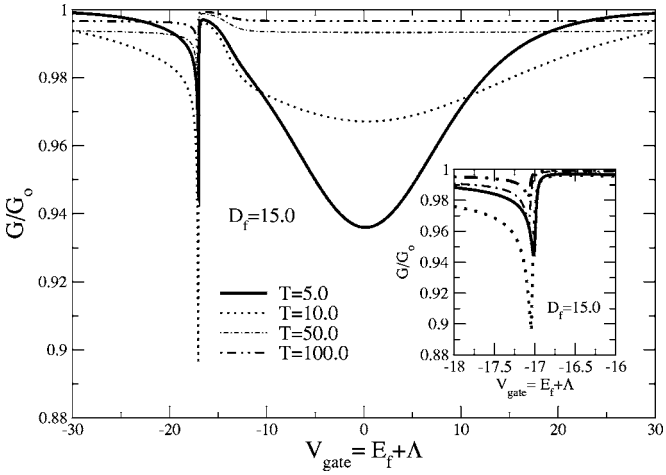

FIG. 6. Conductance G vs $\tilde{E_f}$ for several temperatures (high temperature behavior).

In Fig. 7 we present the behavior of the lateral resonances for different hybridization values, where $V=\sqrt{2W\Delta/\pi}$, $T=5.0$, and $D_f=15.0$. We can see from the figure that fixing the temperature, the Fano character of the resonance increases with the increase of the hybridization.

IV. DISCUSSION

As we pointed out earlier, a side-coupled quantum dot was recently studied experimentally by Kobayashi *et al.*[6] Unfortunately, they limited their study to very low temperatures in order to be able to study the Fano-Kondo antiresonances. Our purpose here is to analyze a similar device but for higher temperature. Let us suppose that the two-dimensional electronic gas of the system presents a carrier density $\rho_c=3.8\times10^{10}$ cm^{-2}. As the 2D density of states in these systems is $\rho_E=\frac{m^*}{\pi h^2}$, where m^* is the electronic effective mass (we suppose the system to be made of GaAs) and h is Planck's constant, it is possible to estimate the value of the chemical potential μ measured from the bottom of the conduction band $D_f\approx1.0$ meV. This result implies that the Fano antiresonance we are studying could already appear for temperatures $T\approx5$ K. On the other hand, several meV for the QD interlevel spacing is an attainable experimental condition.

V. SUMMARY AND CONCLUSIONS

In this work we have studied the transport properties of a T-shaped quantum dot in the strong coupling regime, applying the X-boson method for the single-impurity case, in the limit of $U\to\infty$. We observe that when the $\tilde{E_f}$ localized level is located near the edge of the CB a lateral Fano resonance appear. At low temperatures, there is a Fano lateral resonance associated to the Kondo effect, for a QD populated by an odd number of electrons. This is an experimentally well studied phenomenon. As the temperature is increased above the Kondo temperature this Kondo-Fano antiresonance disap-

pears and, according to our results, another type of Fano behavior dominates the conductance when the gate potential is at the neighborhood of the bottom of the CB. This new Fano structure is a result of the quantum interference between the ballistic channel and the thermal activated channel created by the discrete resonance at the edge of the CB. We would like to emphasize that this type of Fano resonance is enhanced when the QD is connected to a one-dimensional lead. The Van Hove singularities at the edge of the CB strongly hybridize the *f* level, amplifying the Fano effect. We expect that a possible experimental realization of this Fano resonance could be obtained in devices where the ballistic channel is constituted by a carbon nanotube,[22–25] because the DOS, in this class of materials, presents several Van Hove singularities that can amplify the Fano effect.

To the best of our knowledge, this Fano regime has not been experimentally studied so far. We hope that our results will motivate experimental investigations of this Fano behavior.

ACKNOWLEDGMENTS

We acknowledge fruitful discussions with S. S. Makler, financial support from the Brazilian agencies CNPq and FAPERJ, grant "Primeiros Projetos," CAPES, and the Latin-American institution CLAF.

*Electronic address: figueira@if.uff.br

[1] K. Kang, S. Y. Cho, J. J. Kim, and S. C. Shin, Phys. Rev. B **63**, 113304(R) (2001).
[2] A. A. Aligia and C. R. Proetto, Phys. Rev. B **65**, 165305 (2002).
[3] M. A. Davidovich, E. V. Anda, C. A. Busser, and G. Chiappe, Phys. Rev. B **65**, 233310 (2002).
[4] M. E. Torio, K. Hallberg, A. H. Ceccatto, and C. R. Proetto, Phys. Rev. B **65**, 085302 (2002).
[5] R. Franco, M. S. Figueira, and E. V. Anda, Phys. Rev. B **67**, 155301 (2003).
[6] Kensuke Kobayashi, Hisashi Aikawa, Akira Sano, Shingo Katsumoto, and Yasuhiro Iye, Phys. Rev. B **70**, 035319 (2004).
[7] J. Göres, D. Goldhaber-Gordon, S. Heemeyer, M. A. Kastner, H. Shtrikman, D. Mahalu, and U. Meirav, Phys. Rev. B **62**, 2188 (2000).
[8] M. Madhavam, W. Chen, T. Jamneala, M. F. Crommie, and N. S. Wingreen, Science **280**, 567 (1998); J. Li, W. D. Schneider, R. Berndt, and B. Delley, Phys. Rev. Lett. **80**, 2893 (1998).
[9] L. I. Glazman and V. Chandrasekar, Europhys. Lett. **19**, 623 (1992); T. K. Ng and P. A. Lee, Phys. Rev. Lett. **61**, 1768 (1988); L. I. Glazman and M. E. Raikh, JETP Lett. **47**, 452 (1988); S. Hershfield, J. H. Davies, and J. W. Wilkins, Phys. Rev. Lett. **67**, 3720 (1991); Y. Meir, N. S. Wingreen, and P. A. Lee, *ibid.* **70**, 2601 (1993); N. S. Wingreen and Y. Meir, Phys. Rev. B **49**, 11040 (1994); M. A. Davidovich, E. V. Anda, J. R. Iglesias, and G. Chiappe, Rapid Commun. Mass Spectrom. **55**, R7335 (1997).
[10] D. Goldhaber-Gordon, J. Gores, M. A. Kastner, H. Shtrikman, D. Mahalu, and U. Meirav, Phys. Rev. Lett. **81**, 5225 (1998).
[11] U. Fano, Phys. Rev. **15**, 1966 (1961).
[12] W. Hofstetter, J. Konig, and H. Schoeller, Phys. Rev. Lett. **87**, 156803 (2001).
[13] I. G. Zacharia, D. Goldhaber-Gordon, G. Granger, M. A. Kastner, Y. B. Khavin, H. Shtrikman, D. Mahalu, and U. Meirav, Phys. Rev. B **64**, 155311(R) (2001).
[14] A. A. Aligia and L. A. Salguero, Phys. Rev. B **70**, 075307 (2004).
[15] M. E. Torio, K. Hallberg, S. Flach, A. E. Miroshnichenko, and M. Titov, Eur. J. Biochem. **37**, 399 (2004).
[16] R. Franco, M. S. Figueira, and M. E. Foglio, Phys. Rev. B **66**, 045112 (2002).
[17] R. Franco, M. S. Figueira, and M. E. Foglio, Physica A **308**, 245 (2002).
[18] J. Hubbard, Proc. R. Soc. London, Ser. A **276**, 238 (1964).
[19] M. S. Figueira, M. E. Foglio, and G. G. Martinez, Phys. Rev. B **50**, 17933 (1994).
[20] M. E. Foglio and M. S. Figueira, J. Phys. A **30**, 7879 (1997).
[21] M. E. Foglio and M. S. Figueira, Int. J. Mod. Phys. B **12**, 837 (1998).
[22] D. Goldhaber-Gordon, J. Göres, M. A. Kastner, H. Shtrikman, D. Mahalu, and U. Meirav, Phys. Rev. Lett. **81**, 5225 (1998).
[23] R. M. Konik, cond-mat/0401617 (unpublished).
[24] B. R. Bulka and P. Stefanski, Phys. Rev. Lett. **86**, 5128 (2001).
[25] R. Saito, G. Dresselhaus, and M. S. Dresselhaus, *Physical Properties of Carbon Nanotubes* (Imperial College Press, FL, 1998).